NASA TN D-1295

TECHNICAL NOTE

D-1295

RE-ENTRY GLIDE MANEUVERS FOR RECOVERY OF A WINGED FIRST-STAGE ROCKET BOOSTER

By Alan D. Levin and Edward J. Hopkins

Ames Research Center
Moffett Field, Calif.

NATIONAL AERONAUTICS AND SPACE ADMINISTRATION

WASHINGTON May 1962

1T

NATIONAL AERONAUTICS AND SPACE ADMINISTRATION

TECHNICAL NOTE D-1295

RE-ENTRY GLIDE MANEUVERS FOR RECOVERY OF A WINGED FIRST-STAGE ROCKET BOOSTER

By Alan D. Levin and Edward J. Hopkins

SUMMARY

A numerical study was made of downrange glide and of banking and looping maneuvers to investigate the effect of lift-drag ratio, bank angle, and ballistic coefficient upon downrange recovery and upon return toward the launch site of a winged first-stage rocket booster. The ranges of the variables considered were lift-drag ratios from 0 to 2.0, ballistic coefficients from 0.10 to 0.50 square foot per slug, and bank angles from 10° to 90°. For any combination of parameters considered, it was found that the winged booster could not be returned to the launch site by unpowered flight alone. When all three maneuvers were combined and for lift-drag ratios up to 6.0 (2.0 while supersonic, 6.0 while subsonic), the maximum maneuver boundary was found to enclose a region extending from 124 to 490 miles downrange from the launch site and up to approximately 125 miles laterally from the launch flight path. These distances are a first-order approximation of the maneuver boundary since the method of analysis did not permit modulating the lift.

INTRODUCTION

The current trend toward larger and more powerful rocket boosters has resulted in very large unit costs. A firing frequency may eventually be reached which will require booster recovery; it is therefore appropriate to consider the problems associated with various recovery techniques.

One possible technique for recovery of a first-stage booster involves the use of wings. Winged recovery is of interest because it offers the potential of either returning to the launch site or gliding to some alternate site.

The objective of the analysis reported herein was to explore the effectiveness of wings to provide a gliding and maneuvering capability as a means of booster recovery. To satisfy this objective, three types of maneuvers were studied: a downrange glide, a banking glide, and a loop glide. The stagnation-point convective heating rates, decelerations, and distance from the launch site accompanying these maneuvers are presented for several values of lift-drag ratio and ballistic coefficient.

The problem of atmosphere entry with orbital velocity has been the subject of considerable study (e.g., see refs. 1 and 2). A spent first-stage rocket booster, however, enters the atmosphere at a much lower velocity and little information has been published on this type of entry.

The rocket vehicle selected for the current investigation was capable of placing 27,000 pounds of useful payload into an orbit 300 nautical miles above the earth's surface. The reductions of the orbital payload capability of a similar booster which result from inert weight added to the first stage, to provide for wings and structural modifications or for other recovery gear, are considered in reference 3.

NOTATION

A	reference area, ft^2
C_D	drag coefficient, $\frac{D}{qA}$
C_L	lift coefficient, $\frac{L}{qA}$
D	drag, lb
g	acceleration of gravity at sea level, ft/sec^2
h	altitude above earth's surface, ft
I_{sp}	specific impulse, sec
L	lift, lb
m	mass, slugs
q	dynamic pressure, $\frac{1}{2}\rho V_a^2$, lb/ft^2
$\dot{q}$	laminar convective heating rate at stagnation point, $Btu/ft^2/sec$
s	range traveled over earth's surface, ft
t	time, sec
V	absolute velocity, ft/sec
V_a	velocity relative to a rotating atmosphere, ft/sec
$\dot{V}$	longitudinal deceleration, ft/sec^2

$V\dot{\gamma}$ normal deceleration, ft/sec^2

$\dot{V}_R$ resultant deceleration, g

β bank angle, deg

γ_a flight-path angle relative to a rotating atmosphere, measured from the local horizontal, positive up, deg

φ latitude, measured from the equator, positive northward, deg

ρ atmospheric density, slugs/ft^3

METHOD OF ANALYSIS

Trajectories

The study of downrange and looping glide maneuvers was based on a two-dimensional analysis while the banking glide maneuver required a three-dimensional analysis. The investigation was conducted on an IBM 704 digital computer, which integrated the equations of motion found in appendix A.

Reference trajectory.- A booster reference trajectory was obtained to prescribe the initial conditions for the entry maneuvers investigated. This reference trajectory was obtained from the launch conditions for placing 27,000 pounds of useful payload into a 300 nautical mile orbit:

1. A 20-second vertical rise time from latitude 28.48° north
2. An impulsive tilt in a due east direction at the end of the vertical rise
3. A gravity turn for the remaining portion of the trajectory
4. No drag from launch, through apogee, to the point of re-entry into the sensible atmosphere
5. The sensible atmosphere was assumed to extend to an altitude of approximately 60 statute miles.

The basis for the assumption of zero drag from launch to the point of re-entry was that during the ascent portion of the trajectory the thrust force is much greater than the drag force, while at the higher altitudes (after booster burnout) the gravitational force is dominant in determining the motion. Calculations further showed that the assumption of zero drag from launch to atmosphere re-entry resulted in about a 4-percent difference in the initial entry conditions obtained with the inclusion of drag.

Re-entry trajectories.- The conditions at booster re-entry into the sensible atmosphere were used as the initial conditions for the re-entry maneuvers studied. The conditions were obtained from the reference trajectory at the beginning of the sensible atmosphere. The basic assumptions made during this portion of the trajectories were:

1. The booster was heading due east at latitude 28.48° north upon entry into the sensible atmosphere.

2. C_DA/m, L/D, and β were constant through a given trajectory.

Parameters and Initial Conditions

Downrange glide.- The downrange glide maneuver was investigated for values of L/D from 0 to 2.0 and for values of C_DA/m from 0.10 to 0.50 $ft^2/slug$. The flight parameters of the booster at initiation of the downrange glide maneuver are given in table I.

Banking glide.- The banking glide maneuver was investigated for values of L/D from 0.5 to 2.0, for a value of $C_DA/m = 0.50$ $ft^2/slug$, and for values of β from 10° to 90°. The initial conditions for this maneuver are given in table I.

Looping glide.- The looping glide maneuver was investigated for values of C_DA/m from 0.10 to 0.50 $ft^2/slug$ and for values of L/D from 2.0 to 6.0. For this maneuver the parametric variation of C_DA/m was initiated at the beginning of the sensible atmosphere. A lift-drag ratio of 2.0 was applied at the conditions listed in table I in order to initiate the pullup. At the top of the loop (a flight-path angle of 180°) the booster was assumed to be instantaneously rolled to an upright position. At this point L/D was varied parametrically to obtain the return distance.

ROCKET VEHICLE CHARACTERISTICS

The characteristics of the rocket vehicle used throughout the analysis are presented in table II. The weights presented are for the individual stages and do not include the upper stage weights.

RESULTS AND DISCUSSION

Typical time histories of ballistic and lifting entry trajectories are presented in figures 1(a) and 1(b), respectively. From figure 1(b) it can be seen that the booster skipped[1] during the descent, but at no time did it skip out of the sensible atmosphere. For all of the variations in L/D and C_DA/m investigated, the maximum resultant deceleration during the downrange glide maneuver occurred at the onset of the first skip, except for the $L/D = 0$ trajectory.

Presented in figure 2 are parameter limitations for the downrange glide maneuver for several values of resultant deceleration and convective heating rates, and for skipping. Also shown in the figure is a region enclosing the range of parameters examined and reported herein. The parametric variations were extended to higher values of L/D and C_DA/m in order to present a more complete picture of the nature of the range considered as restricted by heating rates, decelerations, and skipping. Shown in the figure are representative skip boundaries, of which there are an infinite number, depending upon the selected density. For any combined value of L/D and C_DA/m lying above the selected curve, the vehicle will skip at that altitude or above. For no skipping L/D and C_DA/m must be changed continuously during the descent in order that the combined values place the vehicle below the skip boundary for that density and altitude.

Shown in figure 3 is an altitude-velocity diagram for several maneuvers. The upper curve represents the condition wherein the weight is balanced by the sum of aerodynamic lift plus centrifugal lift. The representative heating curve shown is for a stagnation-point convective heating rate of 17 $Btu/ft^2/sec$ based on a 1-foot nose radius.

A typical bank trajectory is presented in figure 4. Because of the lateral displacement during the bank maneuver, a turn of as much as 190° was required before the booster had reached a heading in the direction of the launch site. Also shown on the figure is the booster altitude as a function of distance from the launch site for the $L/D = 2.0$ turn maneuver. For all lift-drag ratios investigated the bank trajectories were terminated at the completion of the required turn or at an altitude of 45,000 feet, whichever occurred first. The altitude termination condition was due to a limitation of the computing program.

Presented in figure 5 are typical loop maneuvers for several values of C_DA/m and for a value of $L/D = 2.0$. From this figure it can be seen that a value of C_DA/m greater than 0.40 $ft^2/slug$ was required to successfully complete the loop maneuver at an $L/D = 2.0$.

---

[1]As used herein, a skip is the time rate of change of altitude (dh/dt). When dh/dt went from a negative to a positive value, the booster was considered to have skipped.

The total accessible ground area for the booster recovery, using a combination of all three of the glide maneuvers, is presented in figure 6. The outer boundary was obtained by following an $L/D = 2.0$ trajectory until the booster had decelerated to sonic velocity, and then increasing the L/D to 6.0. From figure 6 it can be seen that increasing the subsonic L/D from 2.0 to 6.0 made the point of closest return about 30 percent nearer to the launch site, while the maximum lateral range was extended by as much as 50 percent. Since the booster had reached subsonic velocity before impact it was felt that lift-drag ratios higher than 2.0 would be possible. The accessible ground area shown in figure 6 is to be regarded as approximate in that the values of L/D, C_DA/m, and bank angle were constant. Modulation of lift will permit increasingly higher C_L as speed decreases and will possibly extend the boundaries outward. For the range of parameters considered, it appears that regardless of the type of power-off glide maneuver employed, the booster cannot be returned to the launch site.

A 5 4 1

Figures 7 through 12, inclusive, present the distance from the launch site, decelerations, stagnation-point convective heating rates, and other pertinent details for the three maneuvers investigated. The details of these figures are discussed in appendix B.

Ames Research Center
National Aeronautics and Space Administration
Moffett Field, Calif., Jan. 8, 1962

APPENDIX A

EQUATIONS OF MOTION

The equations of motion used for the present analysis are presented. The basic assumptions made and information pertinent to the computing programs are given for each set of the equations of motion.

TWO-DIMENSIONAL EQUATIONS OF MOTION

Sketch (a) shows the geometry used in describing the motion of the vehicle. The basic assumptions made in determining the equations of motion are:

1. The earth and atmosphere are radially symmetric.
2. The earth is spherically homogeneous.
3. The earth and atmosphere rotate as one body.

Other information pertinent to this computer program is:

1. Lift-drag ratio and $C_D A/m$ were required to be constants.
2. A routine was available for a step change in L/D once during the trajectory.
3. A flight-path angle of $\pm 90^\circ$ could not be used since the computer was required to evaluate the tangent of the flight-path angle.

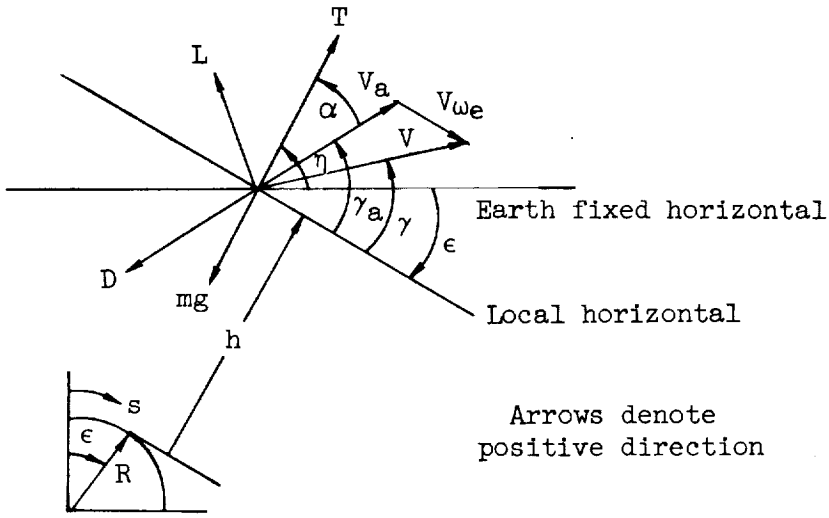

Sketch (a)

Equations (A1) to (A4) are dynamic and kinematic relations which apply to the motion of a particle in a plane under the influence of thrust, drag, lift, and gravitational forces.

$$mV\dot{\gamma} = T \sin(\alpha + \gamma_a - \gamma) - \frac{1}{2} \rho V_a^2 C_D A \sin(\gamma_a - \gamma) + \frac{1}{2} \rho V_a^2 \frac{L}{D} C_D A \cos(\gamma_a - \gamma) + \left(\frac{mV^2}{R + h} - mg\right) \cos \gamma \tag{A1}$$

$$m\dot{V} = T \cos(\alpha + \gamma_a - \gamma) - \frac{1}{2} \rho V_a^2 C_D A \cos(\gamma_a - \gamma) - \frac{1}{2} \rho V_a^2 \frac{L}{D} C_D A \sin(\gamma_a - \gamma) - mg \sin \gamma \tag{A2}$$

A 5 4 1

$$\dot{h} = V \sin \gamma \tag{A3}$$

$$\dot{s} = \frac{R}{R + h} V \cos \gamma - R\omega_e \tag{A4}$$

A dot over a quantity denotes the time rate of change.

The following relations were also required for the program:

$$V_a^2 = V^2 - 2VV_{\omega_e} \cos \gamma + V_{\omega_e}^2 \tag{A5}$$

$$V^2 = V_a^2 + 2V_a V_{\omega_e} \cos \gamma_a + V_{\omega_e}^2 \tag{A6}$$

$$\alpha = \eta + \epsilon - \gamma_a \tag{A7}$$

$$\tan \gamma = \frac{V_a \sin \gamma_a}{V_a \cos \gamma_a + V_{\omega_e}} \tag{A8}$$

$$\tan \gamma_a = \frac{V \sin \gamma}{V \cos \gamma - V_{\omega_e}} \tag{A9}$$

$$\epsilon = \frac{s}{R} \tag{A10}$$

The easterly velocity component due to the earth's rotation is given approximately by

$$V_{\omega_e} = (R + h)\omega_e \cos i \tag{A11}$$

where

i inclination of the orbital plane to the equatorial plane, deg

R earth's radius, ft

T thrust, lb

V_{ω_e} velocity component due to the earth's rotation, ft/sec

α thrust vectoring angle, deg

γ absolute flight-path angle, deg

ϵ range angle, deg

η angle between thrust vector and earth fixed horizontal, deg

ω_e earth's angular velocity, radians/sec

Other symbols used in the equations have been previously defined in the section entitled "Notation."

THREE-DIMENSIONAL EQUATIONS OF MOTION

Sketches (b) through (e) show the geometry used in obtaining the equations of motion for the three-dimensional case. Since this program was used only for re-entry glide maneuvers, the thrust term has been omitted.

The basic assumptions made were:

1. The earth and atmosphere rotate as one body.
2. The earth is oblate.
3. The gravitational potential retained only the terms to the order J (ref. 4).

Other information pertinent to this computing program is:

1. A 1958 ARDC atmosphere, modified by satellite data (ref. 5).
2. L/D, C_DA/m and bank angle are constants.

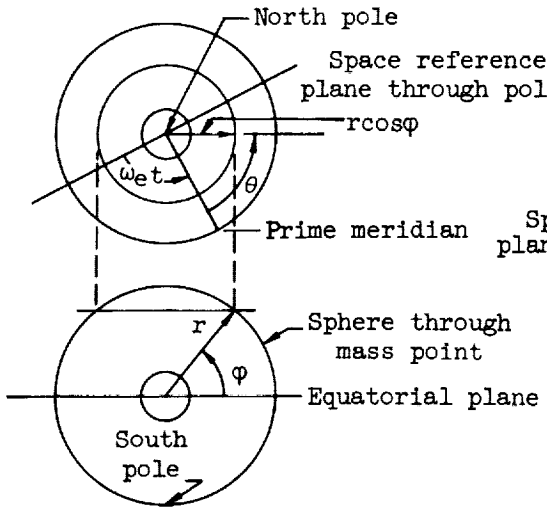

Sketch (b)

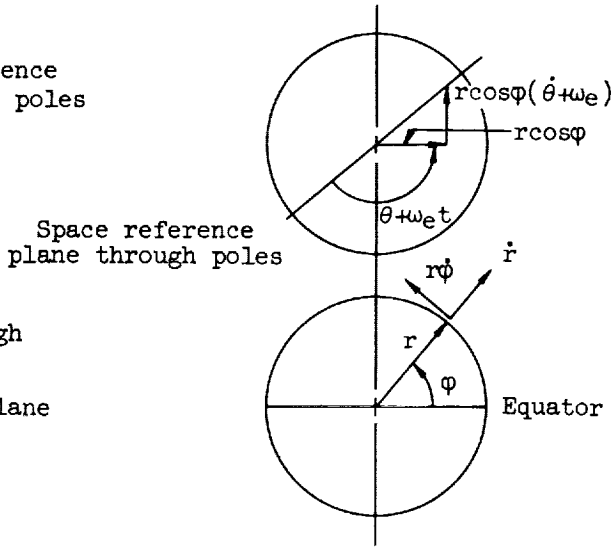

Sketch (c)

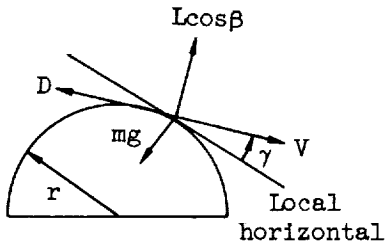

View of great circle plane through V

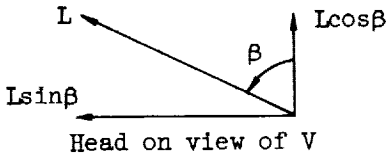

Sketch (d)

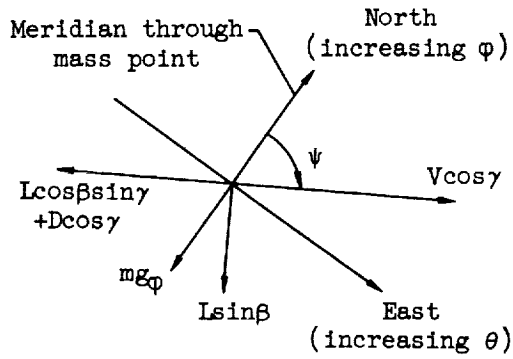

Great circle plane through V
Looking toward earth's center

Sketch (e)

The equations of motion are

$$m[\ddot{r} - r\dot{\varphi}^2 - r\cos^2\varphi(\dot{\theta} + \omega_e)^2] = F_r \qquad \text{(A12)}$$

$$m\left[\frac{1}{r}\frac{d}{dt}(r^2\dot{\varphi}) + r\cos\varphi\sin\varphi(\dot{\theta} + \omega_e)^2\right] = F_\varphi \qquad \text{(A13)}$$

$$m\left\{\frac{1}{r\cos\varphi}\frac{d}{dt}[r^2\cos^2\varphi(\dot{\theta} + \omega_e)]\right\} = F_\theta \qquad \text{(A14)}$$

A 5 4 1

The following relations were also used in the analysis:

$$V = (\dot{r}^2 + r^2\dot{\varphi}^2 + r^2\dot{\theta}^2\cos^2\varphi)^{1/2} \tag{A15}$$

$$F_r = L\cos\beta\cos\gamma - D\sin\gamma - mg_r \tag{A16}$$

$$F_\theta = L\sin\beta\cos\psi - (L\cos\beta\sin\gamma + D\cos\gamma)\sin\psi \tag{A17}$$

$$F_\varphi = -L\sin\beta\sin\psi - (L\cos\beta\sin\gamma + D\cos\gamma)\cos\psi - mg_\varphi \tag{A18}$$

$$U = -\frac{\mu}{r}\left[1 - \frac{J}{3}\left(\frac{R_e}{r}\right)^2(3\sin^2\varphi - 1)\right] \tag{A19}$$

$$g_r = \frac{\partial U}{\partial r} = +\frac{\mu}{r^2}\left[1 - J\left(\frac{R_e}{r}\right)^2(3\sin^2\varphi - 1)\right] \tag{A20}$$

$$g_\varphi = \frac{1}{r}\frac{\partial U}{\partial \varphi} = +\frac{\mu}{r^2}J\left(\frac{R_e}{r}\right)^2\sin 2\varphi \tag{A21}$$

$$h = r - r_\varphi \tag{A22}$$

$$r_\varphi = R_e\left[\cos^2\varphi + \left(\frac{R_e}{R_p}\right)^2\sin^2\varphi\right]^{-1/2} \tag{A23}$$

$$\sin\gamma = \frac{\dot{r}}{V} \tag{A24}$$

$$\psi = \cos^{-1}\left(\frac{r\dot{\varphi}}{V\cos\gamma}\right) = \sin^{-1}\left(\frac{r\dot{\theta}\cos\varphi}{V\cos\gamma}\right) = \tan^{-1}\left(\frac{\dot{\theta}\cos\varphi}{\dot{\varphi}}\right) \tag{A25}$$

where

g_r radial component of earth's gravity, ft/sec^2

g_φ latitude component of earth's gravity, ft/sec^2

J coefficient of the second harmonic in the gravitational potential function

r radius vector, measured from the center of the earth, ft

r_φ radius of the earth at latitude φ, ft

R_e equatorial radius of the earth, ft

R_p polar radius of the earth, ft

U gravitational potential function, ft^2/sec^2

θ earth referenced longitude, measured from the prime meridian, positive eastward, deg

ψ azimuth angle of the earth referenced velocity, measured from local north, deg

μ universal gravitational constant times mass of the earth, ft^3/sec^2

Other symbols used are defined either in the section entitled "Notation" or in the presentation of the two-dimensional equations of motion.

APPENDIX B

GLIDE MANEUVER DETAILS

DOWNRANGE GLIDE

Presented in figures 7(a) to 7(d) are the maximum decelerations, distance from the launch site, heating rates, and dynamic pressure, respectively, for the downrange glide maneuver. The apparent paradox of increasing range with increasing C_DA/m for a constant L/D (except for $L/D = 0$), as indicated in figure 7(b), arises from the booster moving nearer to the skip boundaries and then exceeding them. The tendency to skip resulted from an increase in lift due to an increase in C_DA/m, in order to maintain a constant value of L/D.

BANKING GLIDE

Shown in figures 8 through 10 are details of the banking glide maneuver. The maneuver boundaries shown in figure 10 were obtained by banking the booster until a given heading was reached and then continuing the glide at a constant value of L/D. The over-all recovery areas shown in figure 6 were obtained by a superposition of the individual boundaries shown in figure 10, and combining these with the results from the downrange and looping glide maneuvers.

LOOPING GLIDE

The details of the looping glide maneuver are presented in figures 11 and 12. During the analysis it was discovered that the initiation of the loop was restricted to a range of altitudes between 60,000 and 70,000 feet for an $L/D = 2.0$ and that no loop could be completed at L/D less than 2.0 for the values of C_DA/m investigated. The loop maneuver could not be attempted during the ascent portion of the trajectory because of the low density of the air at and above the altitude for separation of the upper stages from the booster. The maximum heating rates and decelerations for the loop maneuver are presented in figure 11.

Figure 12 presents the distance from the launch site as a function of altitude for $C_DA/m = 0.50$ $ft^2/slug$ and values of L/D ranging from 0 to 6.0. In the figure it can be seen that following the loop the booster skipped for values of L/D equal to or greater than 4.0. It is believed that these skips are not realistic and were a result of the computer program requiring a step change in L/D.

REFERENCES

1. Slye, Robert E.: An Analytical Method for Studying the Lateral Motion of Atmosphere Entry Vehicles. NASA TN D-325, 1960.

2. Rosamond, Daniel L.: Satellite Recovery Techniques for Optimization of Touchdown Accuracy. IAS Paper 59-62, June 1959.

3. Levin, Alan D., and Hopkins, Edward J.: Orbital Payload Reductions Resulting From Booster and Trajectory Modifications for Recovery of a Large Rocket Booster. NASA TN D-1143, 1961.

4. Nielsen, Jack N., Goodwin, Frederick K., and Mersman, William A.: Three-Dimensional Orbits of Earth Satellites, Including Effects of Earth Oblateness and Atmospheric Rotation. NASA MEMO 12-4-58A, 1958.

5. Kallmann, H. K., and Juncasa, M. L.: A Preliminary Model Atmosphere Based on Rocket and Satellite Data. The Rand Corp., RM 2286, Oct. 1958. (Also Rand Corp. P-1591, and Jour. of Geophysical Research, vol. 64, no. 6, June 1959, pp. 615-623)

TABLE I.- INITIAL RE-ENTRY CONDITIONS

	Downrange and banking glide	Looping glide
h, ft	318,450	60,450
V, ft/sec	6,600	[a]1,600-2,900
γ_a, deg	-33.0	-53.0
s, mi	210	290

[a]Dependent upon the value of $C_D A/m$.

TABLE II.- ROCKET VEHICLE CHARACTERISTICS

	Stage 1	Stage 2	Stage 3
Gross weight, lb	788,180	230,096	60,000
Fuel weight, lb	697,680	217,770	26,000
Payload weight, lb	---	---	27,000
Empty weight, lb	90,500	12,326	7,000
Weight flow, lb/sec	5,814	1,190	72
Burning time, sec	120	183	---
Sea-level thrust, lb	1,500,000	---	---
Vacuum thrust, lb	1,691,000	363,000	30,000
Sea-level I_{sp}, sec	258	---	---
Vacuum I_{sp}, sec	291	305	417
Diameter, ft	21.42	13.33	10.00

A
5
4
1

(a) Nonlifting; L/D = 0.

Figure 1. Typical booster trajectories during re-entry; $C_D A/m = 0.50$ ft^2/slug.

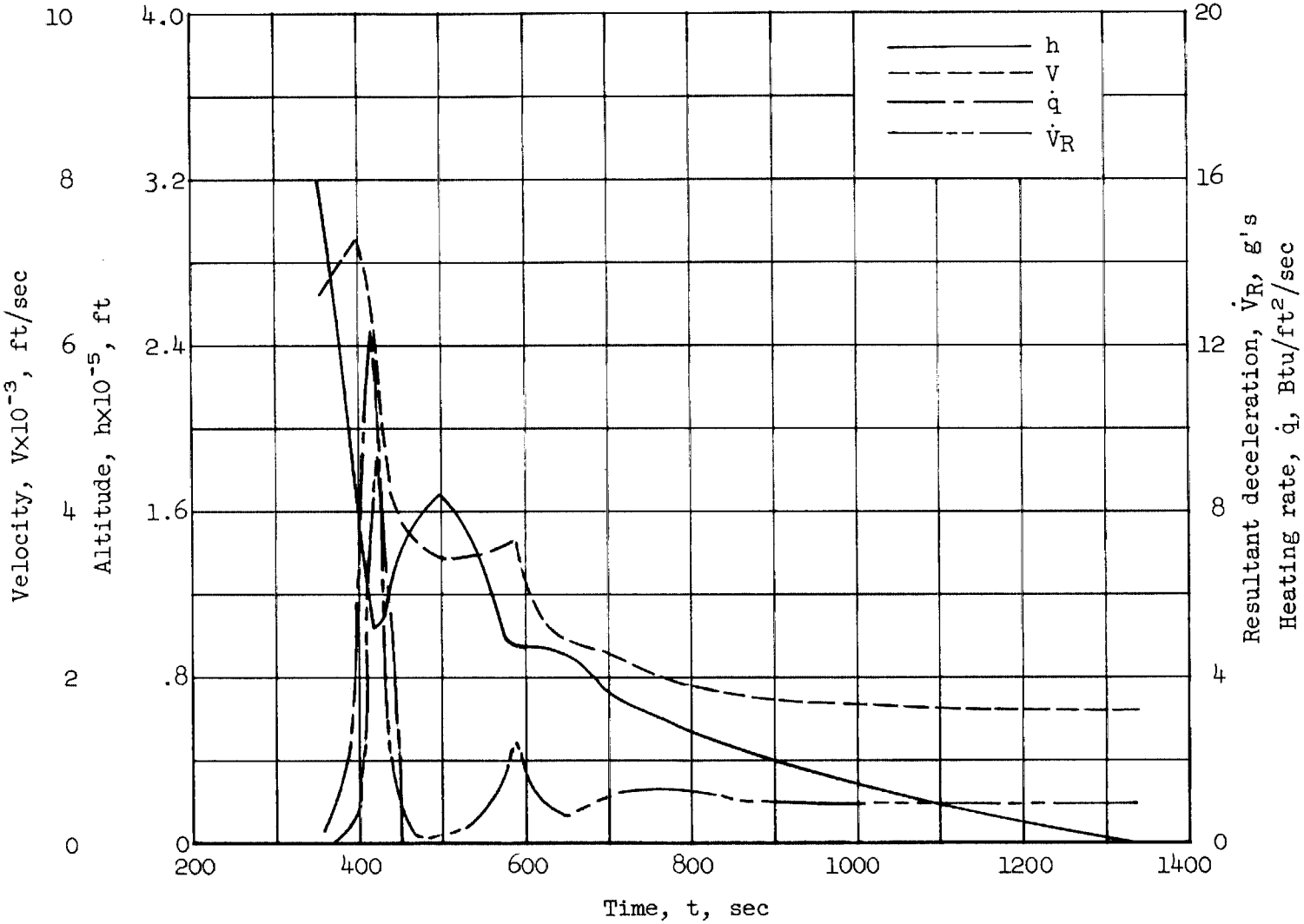

(b) Lifting; L/D = 2.00.

Figure 1.- Concluded.

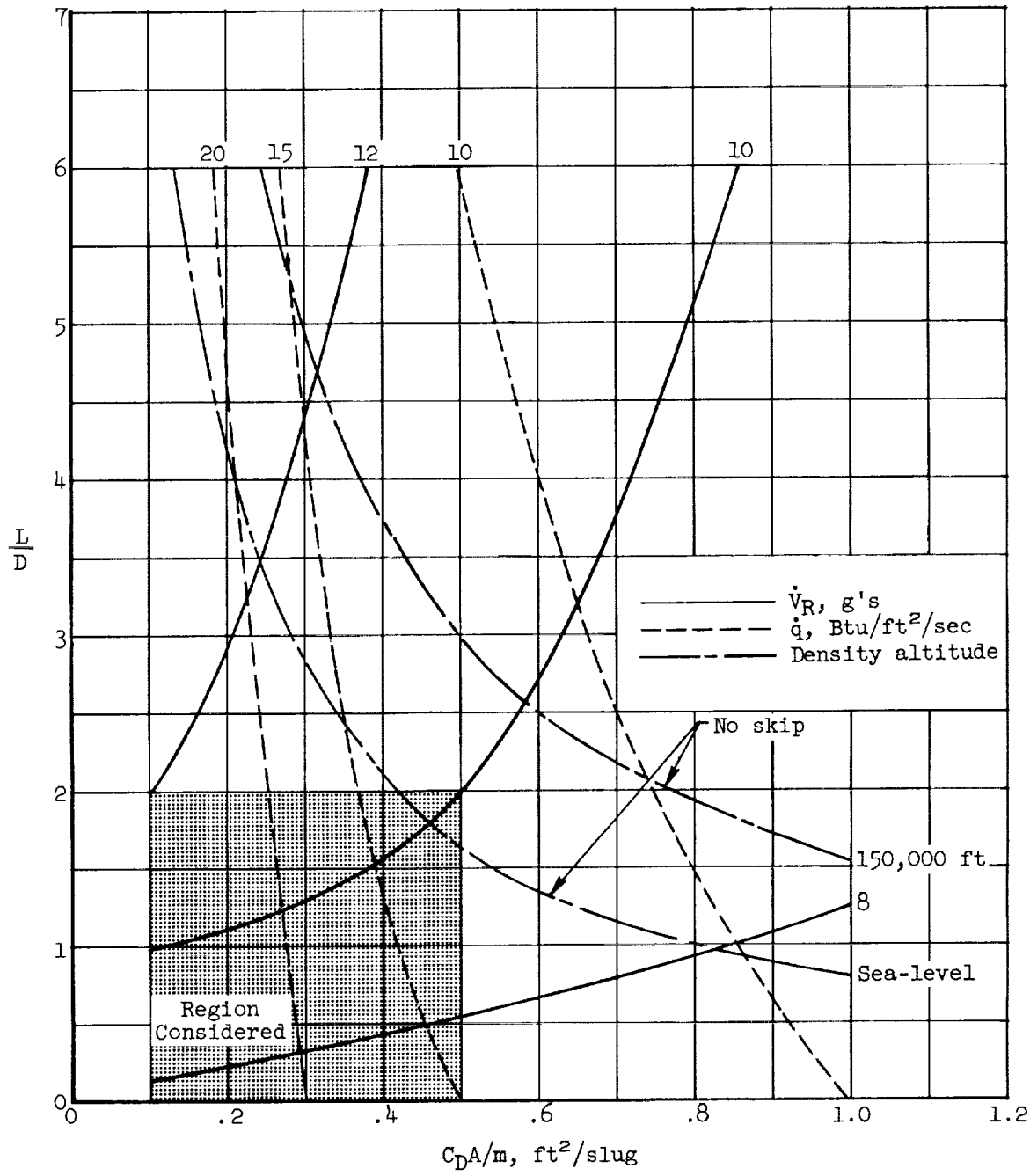

Figure 2.- Parameter limitations for the downrange glide maneuver.

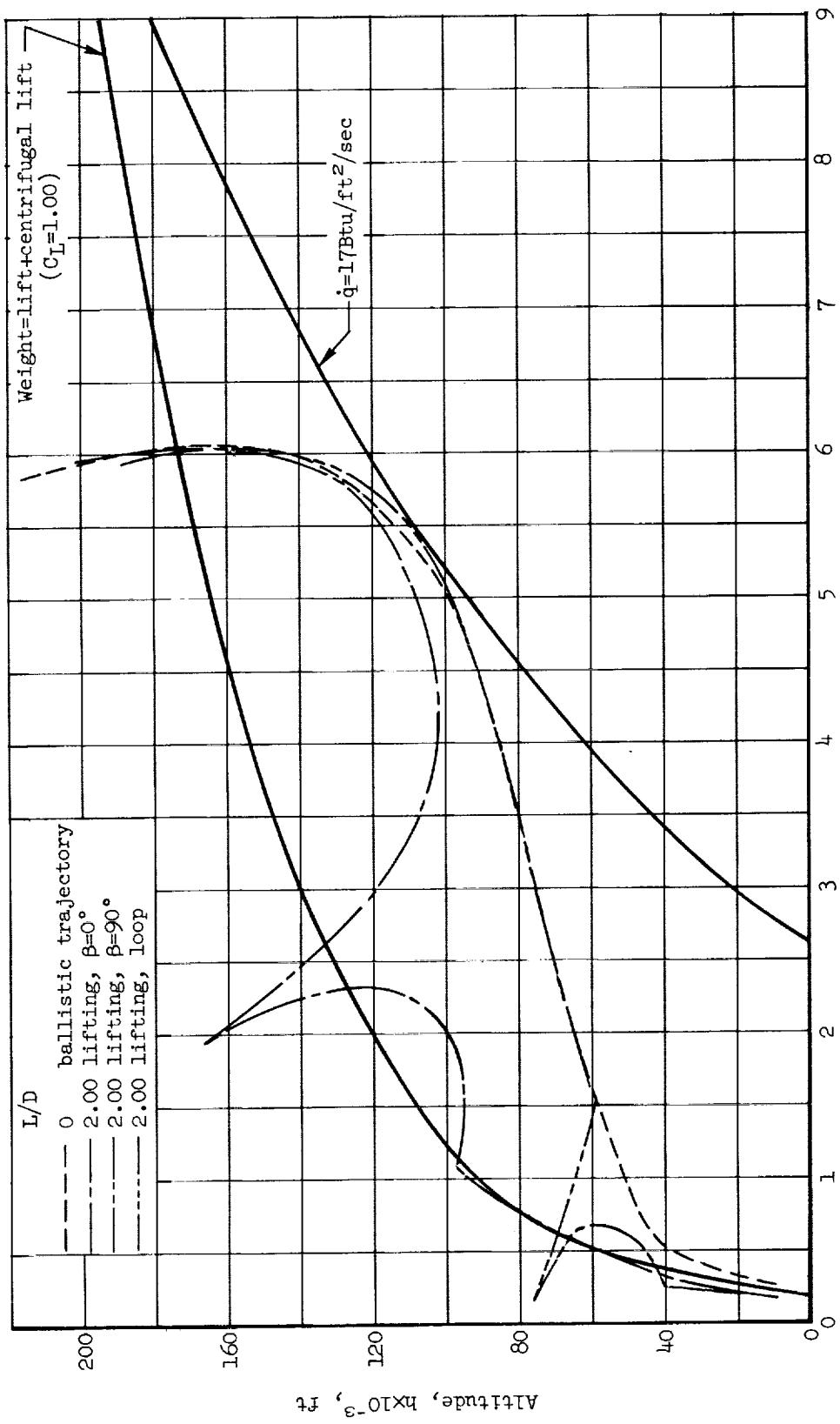

Figure 3.- Velocity-altitude diagram; $C_D A/m$ = 0.50 ft^2/slug.

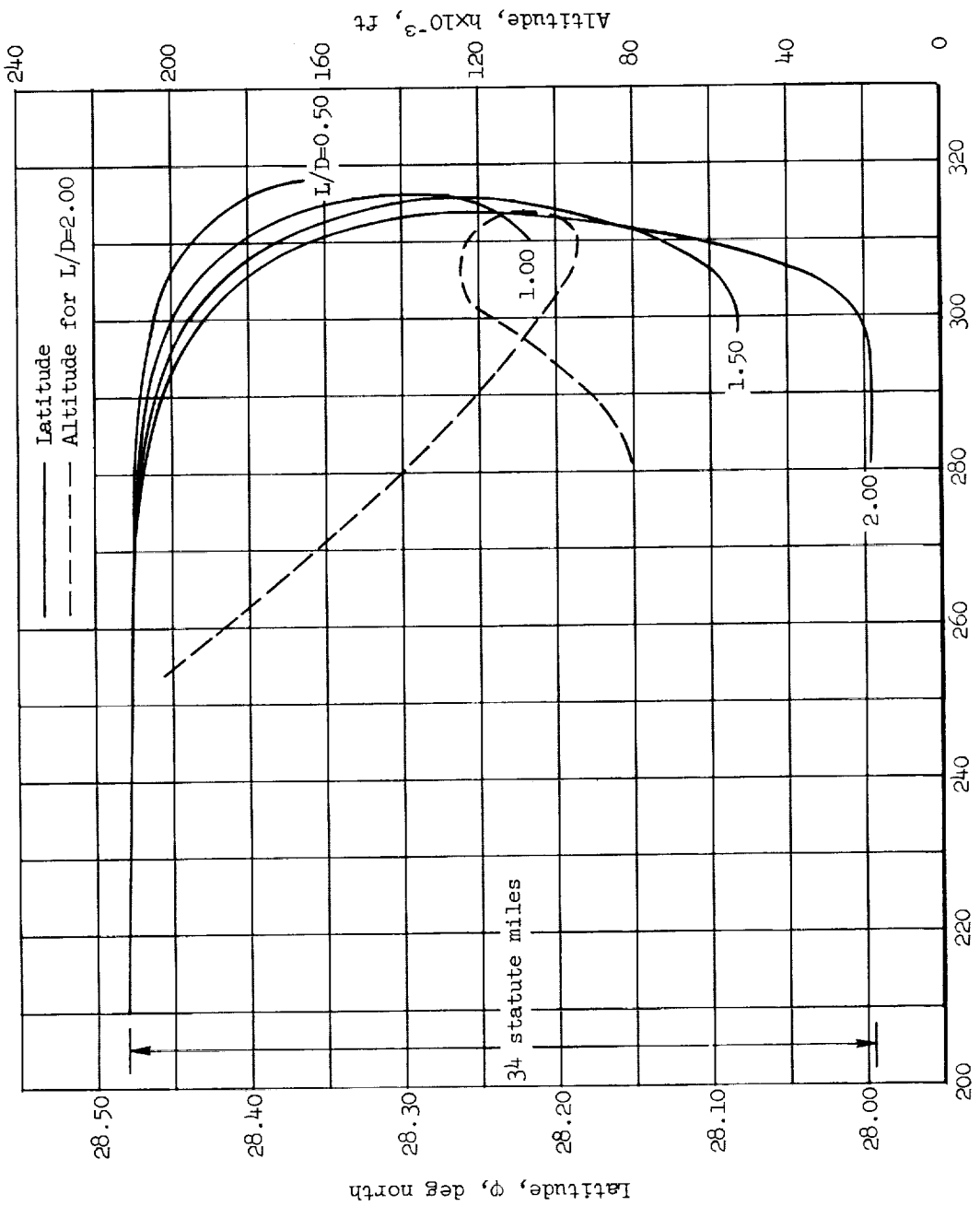

Figure 4.- Typical bank trajectories; $C_D A/m = 0.50$ ft^2/slug, $\beta = 45°$

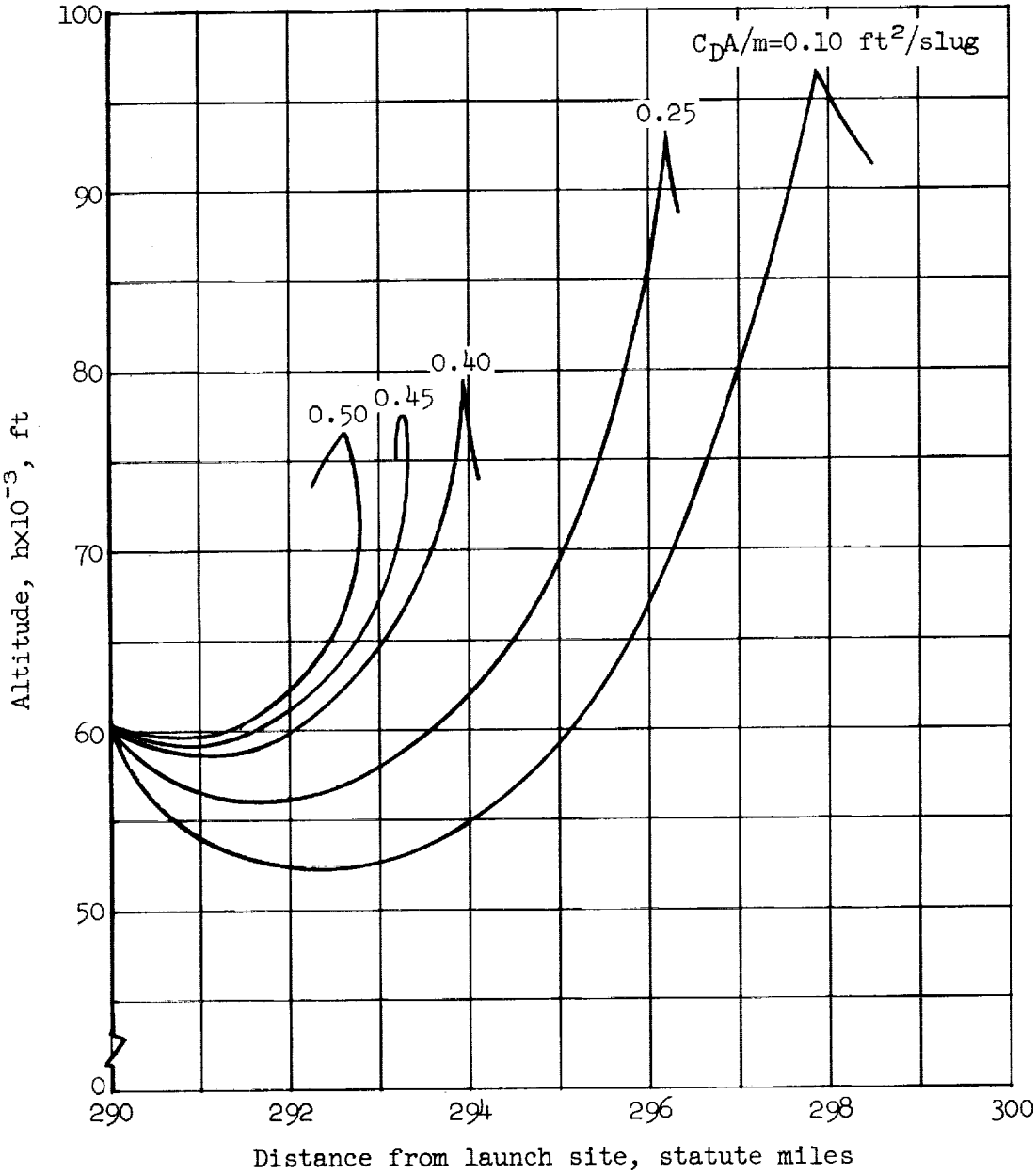

Figure 5.- Effect of ballistic coefficient on the ability to successfully complete the loop maneuver; L/D = 2.00.

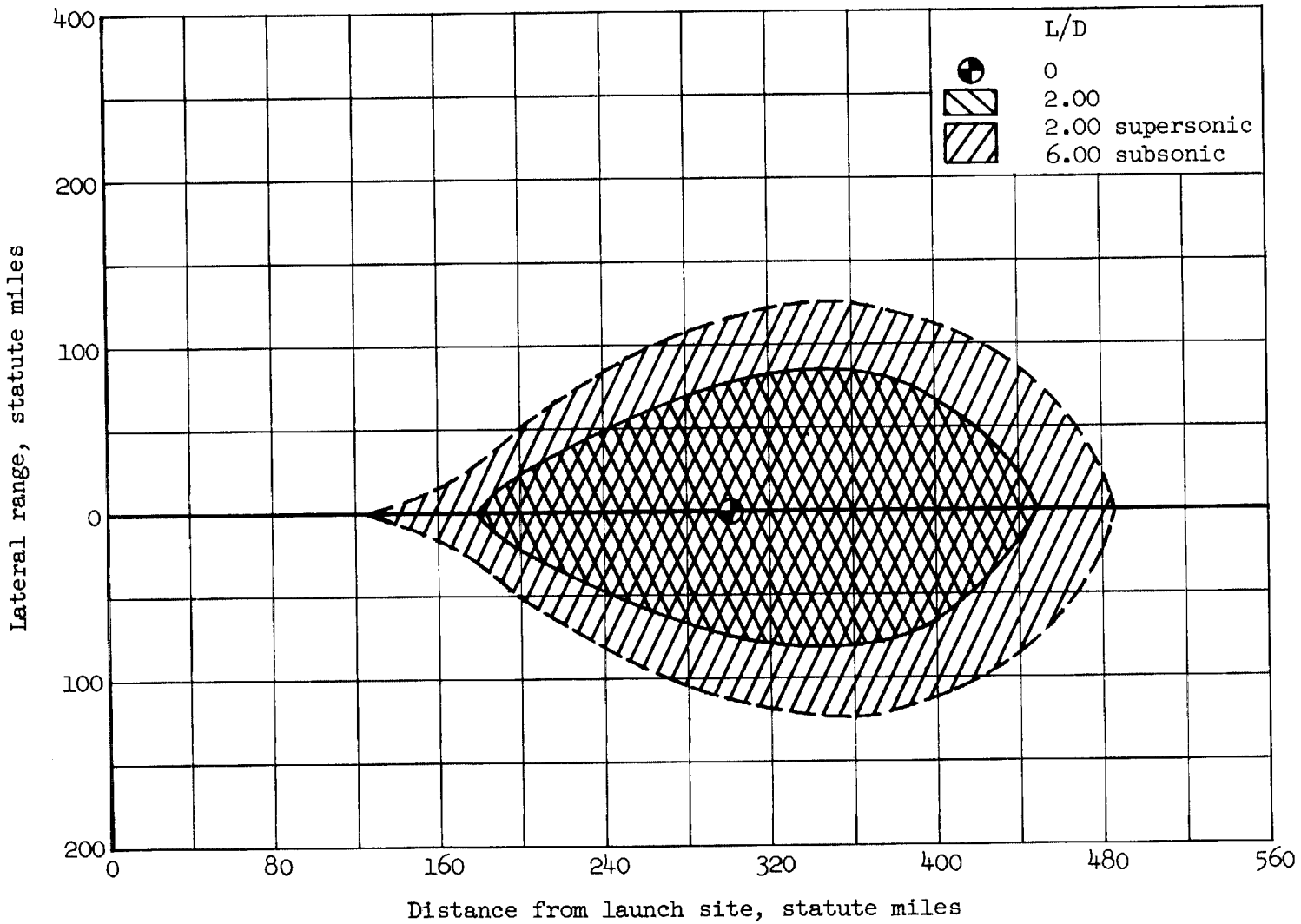

Figure 6.- Total accessible ground area for booster recovery by the use of downrange banking and looping maneuvers; $C_DA/m = 0.50$ ft^2/slug.

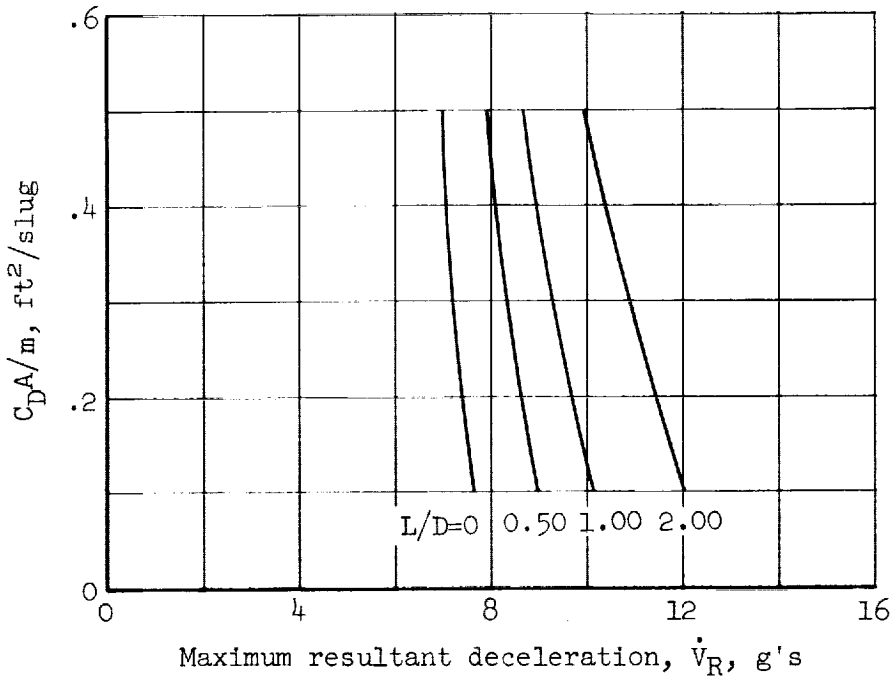

(a) Deceleration.

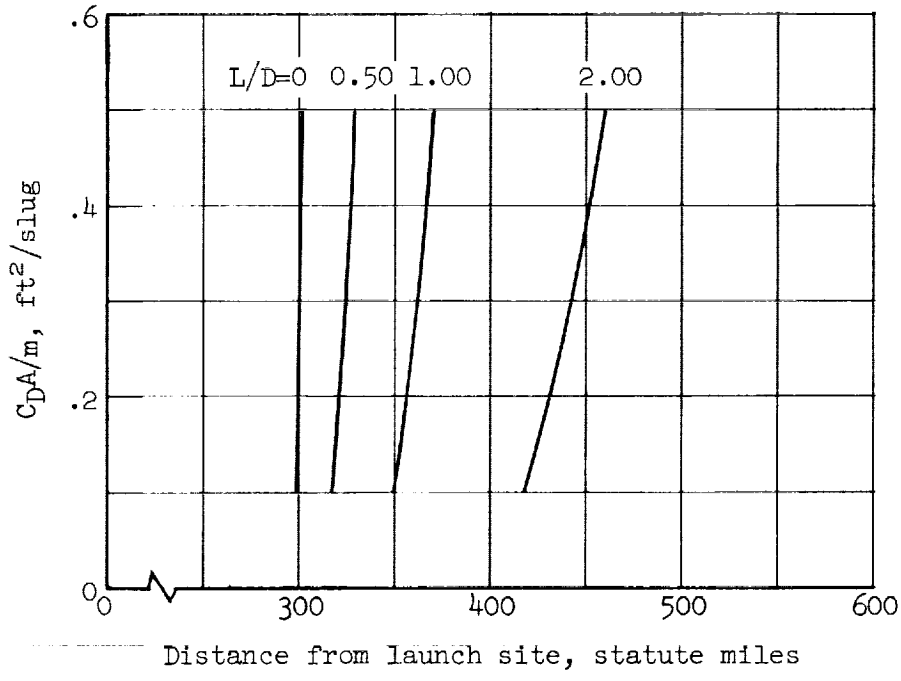

(b) Range.

Figure 7.- Downrange glide maneuver details.

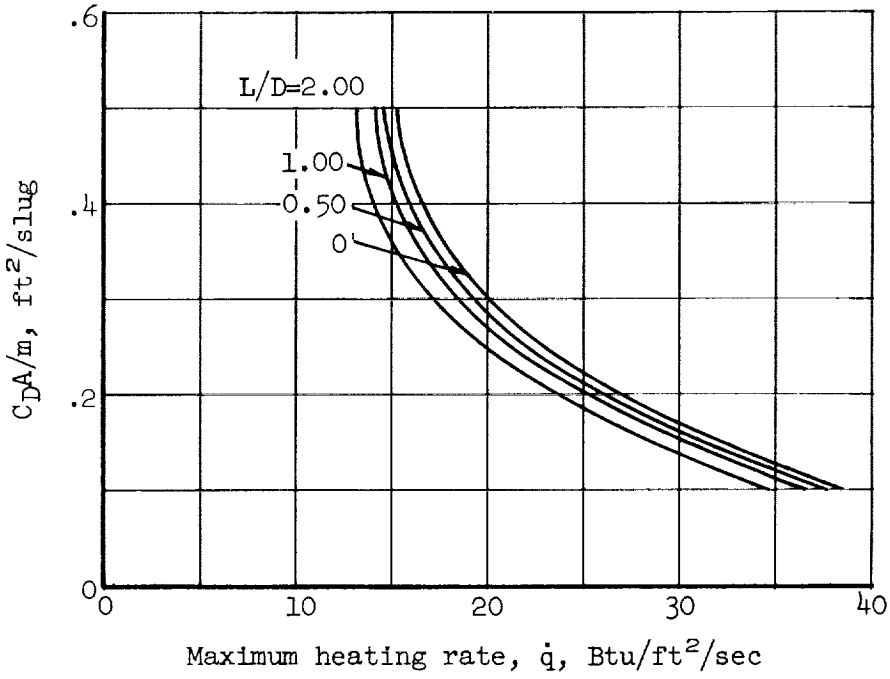

(c) Stagnation-point convective heating rate.

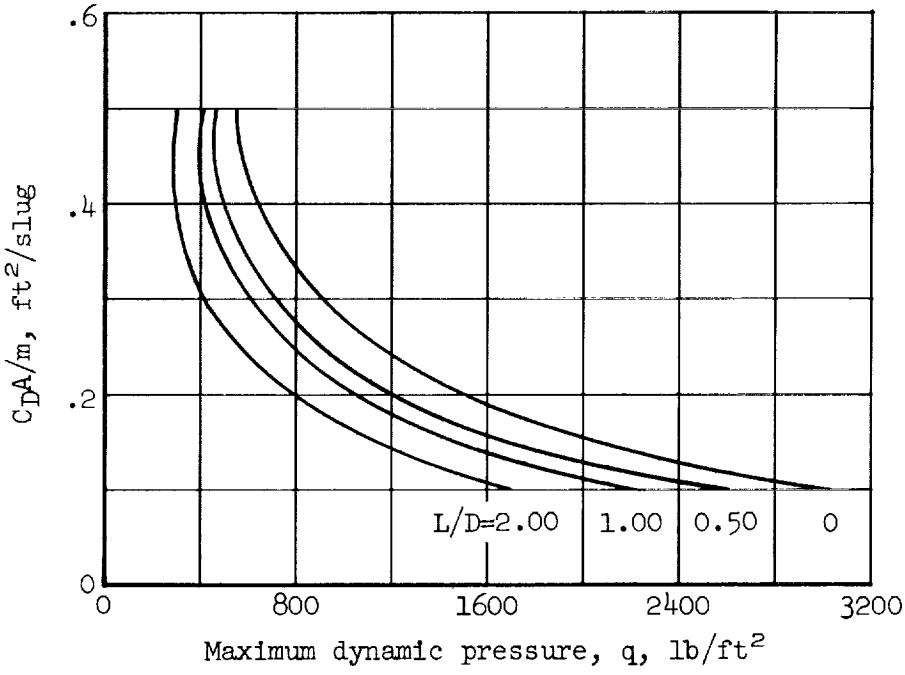

(d) Dynamic pressure.

Figure 7.- Concluded.

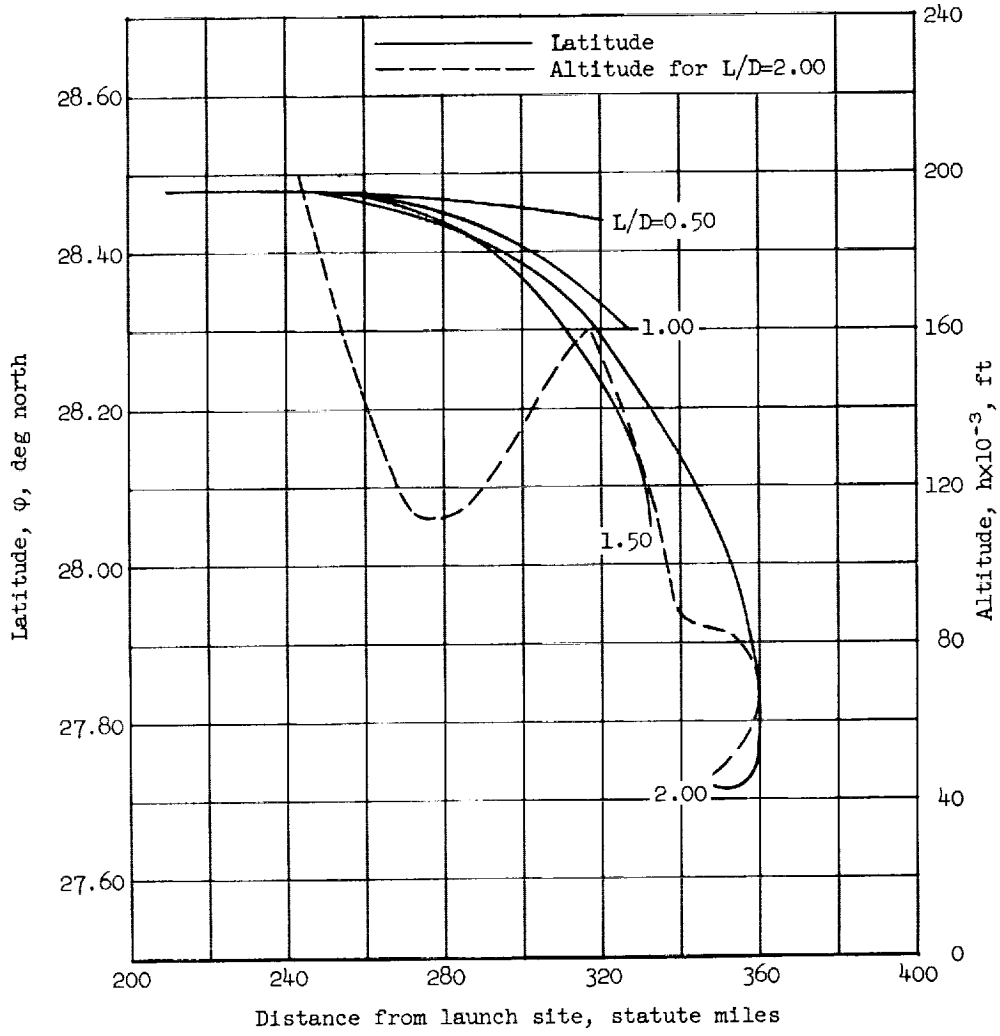

(a) $\beta = 10°$, $C_D A/m = 0.50$ ft^2/slug

Figure 8.- Earth referenced booster coordinates for the banking glide maneuver.

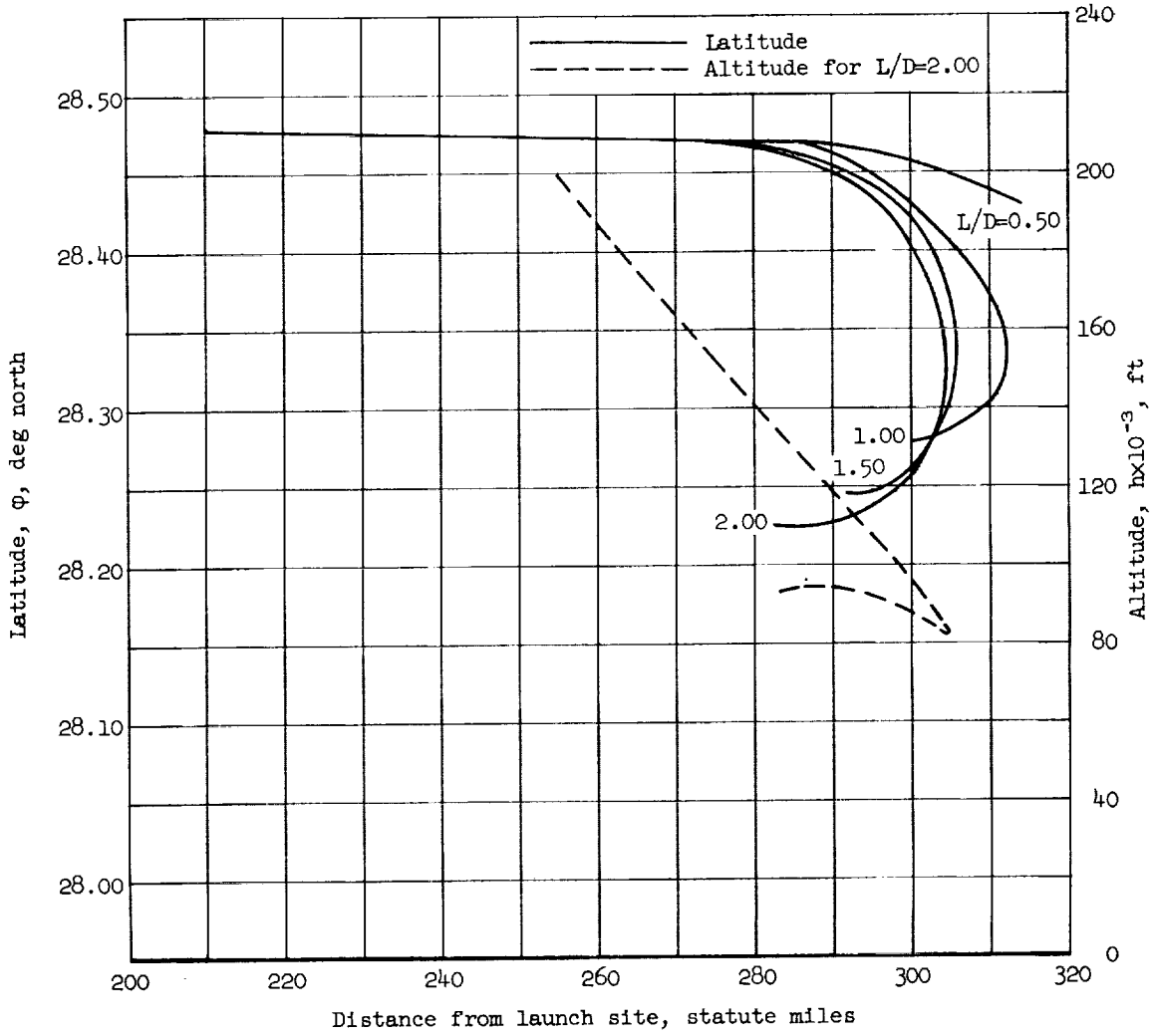

(b) $\beta = 60°$, $C_DA/m = 0.50$ ft^2/slug

Figure 8.- Continued.

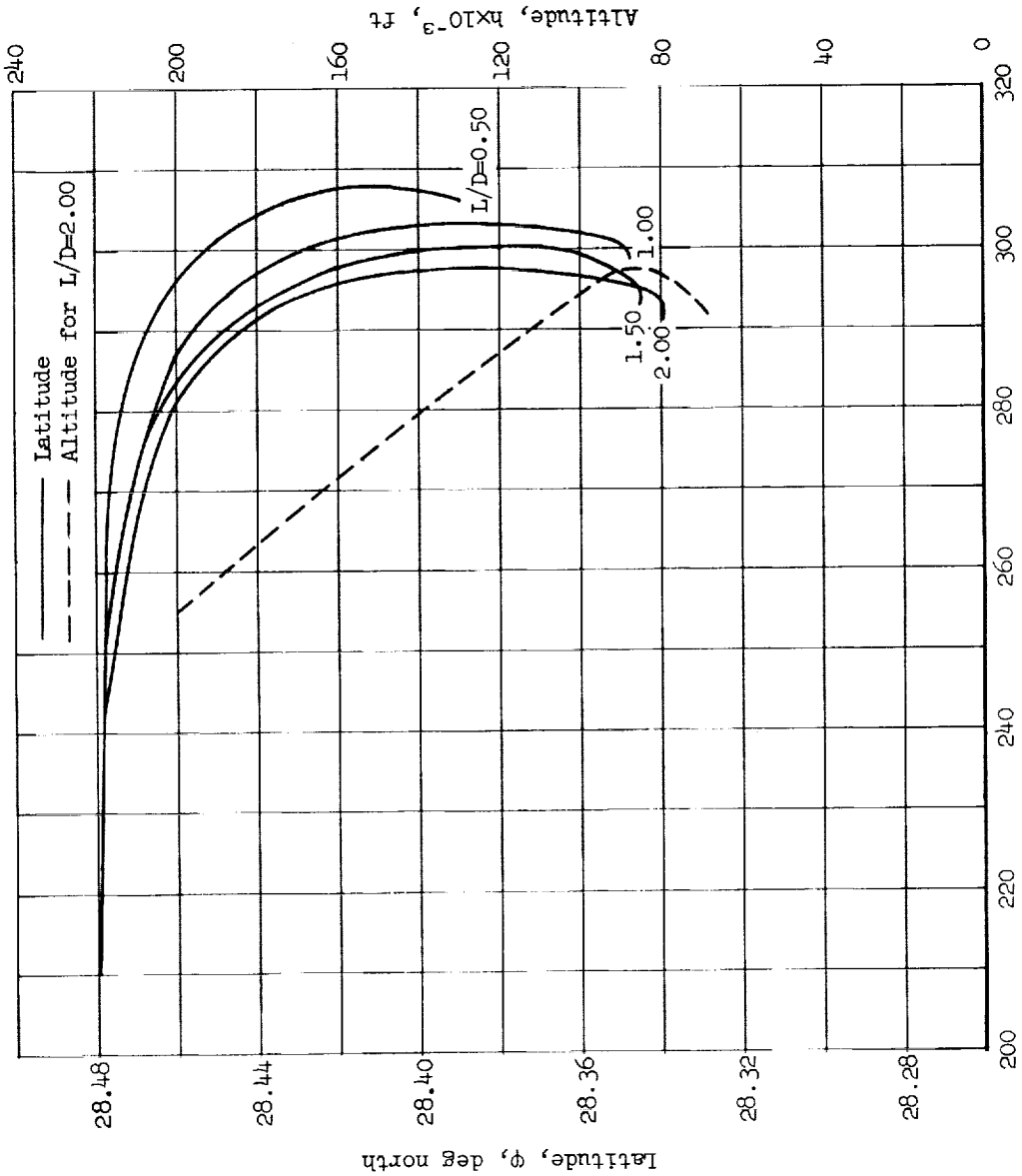

(c) $\beta = 80°$, $C_D A/m = 0.50$ ft^2/slug

Figure 8.- Continued.

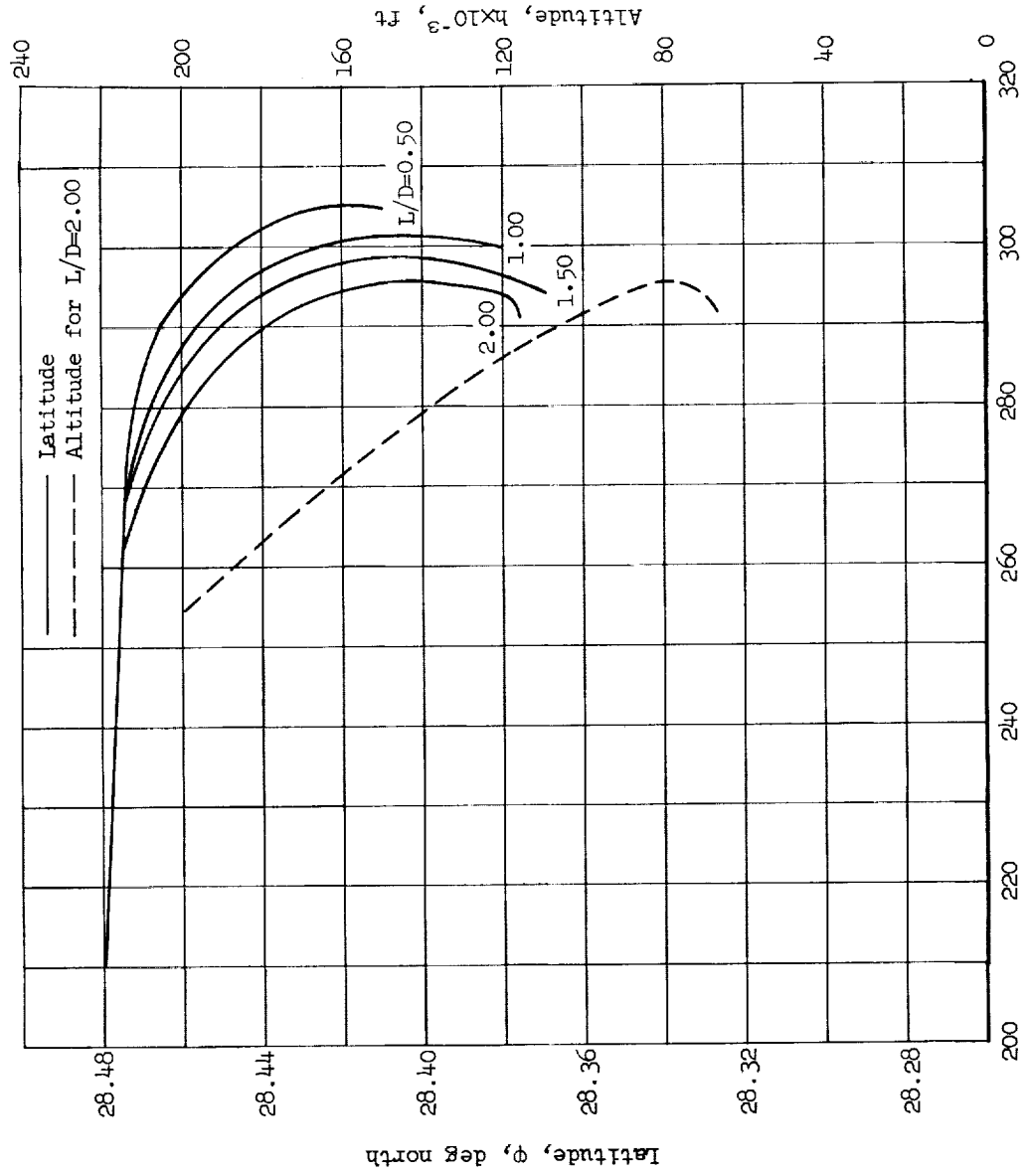

(d) $\beta = 90°$, $C_DA/m = 0.50$ ft^2/slug

Figure 8.- Concluded.

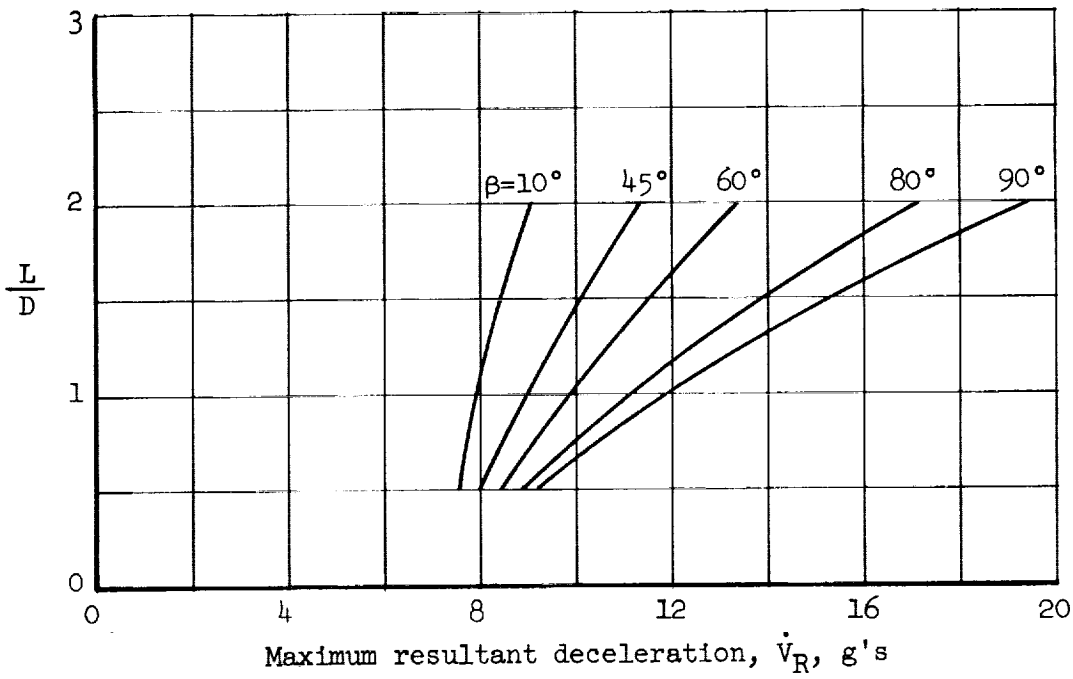

(a) Deceleration.

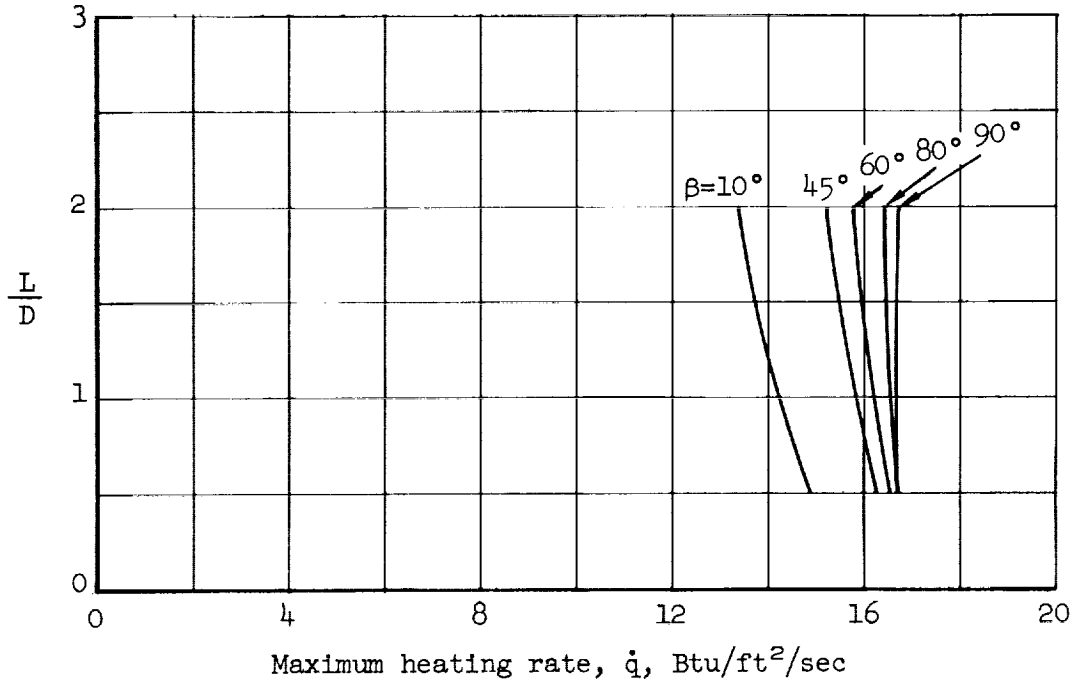

(b) Stagnation-point convective heating rate.

Figure 9.- Banking glide maneuver details; C_DA/m = 0.50 ft^2/slug.

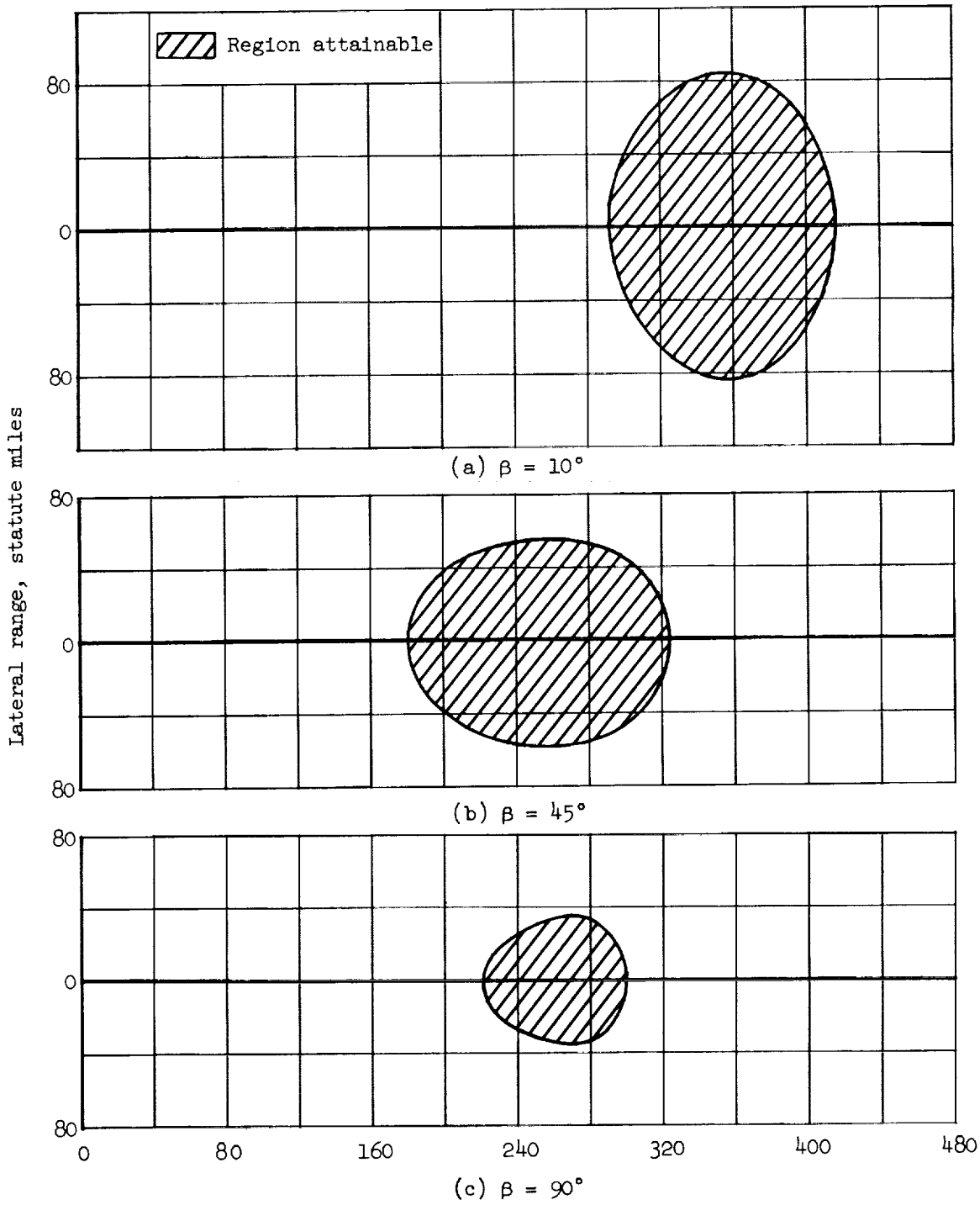

Figure 10.- Ground area attainable with variation of bank angle; L/D = 2.00, C_DA/m = 0.50 $ft^2/slug$.

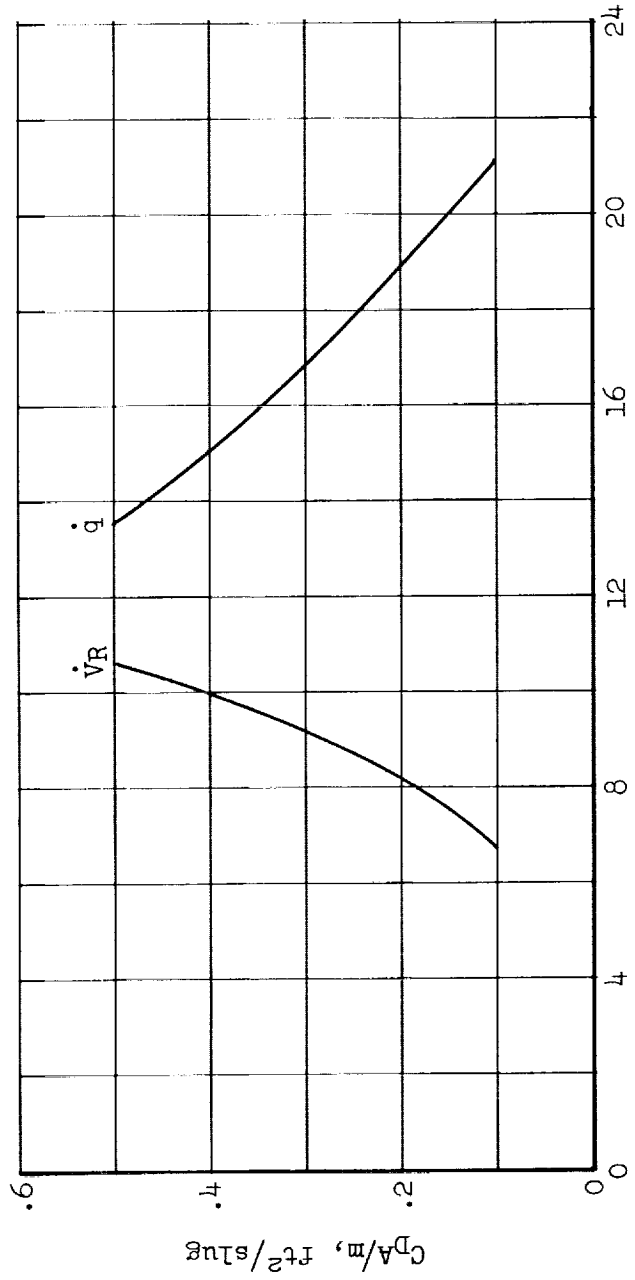

Figure 11.- Looping glide maneuver details; L/D = 2.00

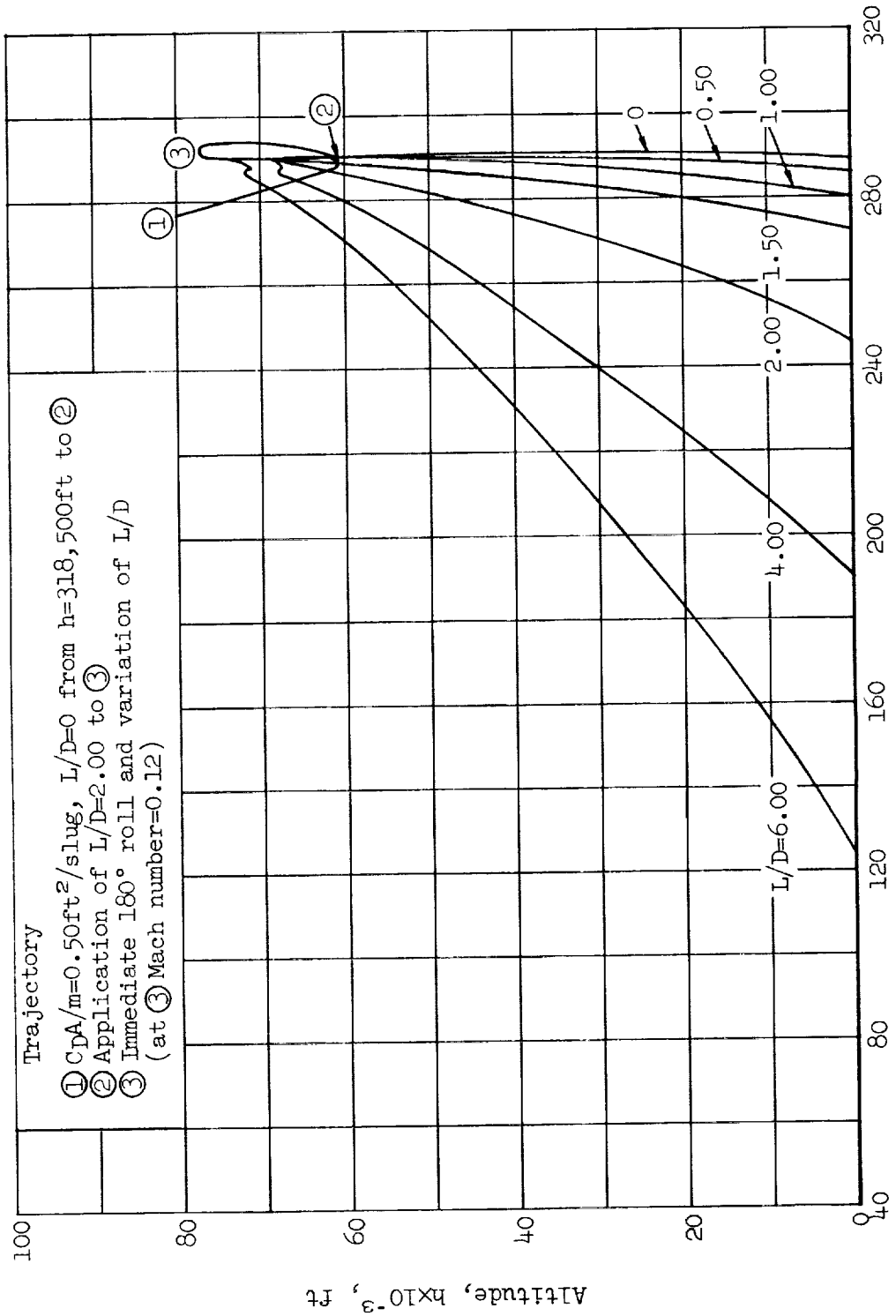

Figure 12.- Effect of lift-drag ratio on the distance from the launch site for the loop-return maneuver.

NASA TN D-1295
National Aeronautics and Space Administration.
RE-ENTRY GLIDE MANEUVERS FOR RECOVERY OF A WINGED FIRST-STAGE ROCKET BOOSTER.
Alan D. Levin and Edward J. Hopkins. May 1962.
33p. OTS price, $1.00.
(NASA TECHNICAL NOTE D-1295)

A study was made of downrange glide and of banking and looping maneuvers to investigate the effect of lift-drag ratio, bank angle, and ballistic coefficient upon the downrange recovery and return to the launch site of a winged first-stage rocket booster. The ranges of the variables considered were lift-drag ratios from 0 to 2.0, ballistic coefficients from 0.10 to 0.50 square foot per slug, and bank angles from 10° to 90°. The results are presented in terms of resultant decelerations, heating rates, and booster recovery area.

I. Levin, Alan D.
II. Hopkins, Edward J.
III. NASA TN D-1295

(Initial NASA distribution: 2, Aerodynamics, missiles and space vehicles; 5, Atmospheric entry; 28, Missiles and satellite carriers.)

NASA

NASA TN D-1295
National Aeronautics and Space Administration.
RE-ENTRY GLIDE MANEUVERS FOR RECOVERY OF A WINGED FIRST-STAGE ROCKET BOOSTER.
Alan D. Levin and Edward J. Hopkins. May 1962.
33p. OTS price, $1.00.
(NASA TECHNICAL NOTE D-1295)

A study was made of downrange glide and of banking and looping maneuvers to investigate the effect of lift-drag ratio, bank angle, and ballistic coefficient upon the downrange recovery and return to the launch site of a winged first-stage rocket booster. The ranges of the variables considered were lift-drag ratios from 0 to 2.0, ballistic coefficients from 0.10 to 0.50 square foot per slug, and bank angles from 10° to 90°. The results are presented in terms of resultant decelerations, heating rates, and booster recovery area.

I. Levin, Alan D.
II. Hopkins, Edward J.
III. NASA TN D-1295

(Initial NASA distribution: 2, Aerodynamics, missiles and space vehicles; 5, Atmospheric entry; 28, Missiles and satellite carriers.)

NASA

NASA TN D-1295
National Aeronautics and Space Administration.
RE-ENTRY GLIDE MANEUVERS FOR RECOVERY OF A WINGED FIRST-STAGE ROCKET BOOSTER.
Alan D. Levin and Edward J. Hopkins. May 1962.
33p. OTS price, $1.00.
(NASA TECHNICAL NOTE D-1295)

A study was made of downrange glide and of banking and looping maneuvers to investigate the effect of lift-drag ratio, bank angle, and ballistic coefficient upon the downrange recovery and return to the launch site of a winged first-stage rocket booster. The ranges of the variables considered were lift-drag ratios from 0 to 2.0, ballistic coefficients from 0.10 to 0.50 square foot per slug, and bank angles from 10° to 90°. The results are presented in terms of resultant decelerations, heating rates, and booster recovery area.

I. Levin, Alan D.
II. Hopkins, Edward J.
III. NASA TN D-1295

(Initial NASA distribution: 2, Aerodynamics, missiles and space vehicles; 5, Atmospheric entry; 28, Missiles and satellite carriers.)

NASA

NASA TN D-1295
National Aeronautics and Space Administration.
RE-ENTRY GLIDE MANEUVERS FOR RECOVERY OF A WINGED FIRST-STAGE ROCKET BOOSTER.
Alan D. Levin and Edward J. Hopkins. May 1962.
33p. OTS price, $1.00.
(NASA TECHNICAL NOTE D-1295)

A study was made of downrange glide and of banking and looping maneuvers to investigate the effect of lift-drag ratio, bank angle, and ballistic coefficient upon the downrange recovery and return to the launch site of a winged first-stage rocket booster. The ranges of the variables considered were lift-drag ratios from 0 to 2.0, ballistic coefficients from 0.10 to 0.50 square foot per slug, and bank angles from 10° to 90°. The results are presented in terms of resultant decelerations, heating rates, and booster recovery area.

I. Levin, Alan D.
II. Hopkins, Edward J.
III. NASA TN D-1295

(Initial NASA distribution: 2, Aerodynamics, missiles and space vehicles; 5, Atmospheric entry; 28, Missiles and satellite carriers.)

NASA